Available online at www.sciencedirect.com
SCIENCE DIRECT®
ELSEVIER
Nuclear Instruments and Methods in Physics Research A 519 (2004) 466–471
NUCLEAR INSTRUMENTS & METHODS IN PHYSICS RESEARCH Section A
www.elsevier.com/locate/nima

Stochastic processes in muon ionization cooling

D. Errede[a,*], K. Makino[a], M. Berz[b], C.J. Johnstone[c], A. Van Ginneken[c]

[a] Department of Physics, University of Illinois at Urbana-Champaign, 1110 W. Green Street, Urbana, IL 61801-3080, USA
[b] Department of Physics and Astronomy, Michigan State University, East Lansing, MI 48824, USA
[c] Fermi National Accelerator Laboratory, P.O. Box 500, Batavia, IL 60510, USA

Abstract

A muon ionization cooling channel consists of three major components: the magnet optics, an acceleration cavity, and an energy absorber. The absorber of liquid hydrogen contained by thin aluminum windows is the only component which introduces stochastic processes into the otherwise deterministic acceleration system. The scattering dynamics of the transverse coordinates is described by Gaussian distributions. The asymmetric energy loss function is represented by the Vavilov distribution characterized by the minimum number of collisions necessary for a particle undergoing loss of the energy distribution average resulting from the Bethe–Bloch formula. Examples of the interplay between stochastic processes and deterministic beam dynamics are given.

1. Introduction

In particle optics, the dynamics is determined by electromagnetic fields, thus it is symplectic. Liouville's theorem guarantees conservation of six-dimensional phase-space density. Relatively new is the inclusion of stochastic phenomena, particles interacting with other particles, such as those needed to describe electron cooling or muon ionization cooling channels [1–5].

A cooling channel is used to manipulate charged particles (muons) such that the four-/six-dimensional-phase space density is increased. Needed are stochastic processes or (outside the realm of classical mechanics) a self-interacting particle such as that in Van der Meer cooling [6]. The cooling channel under consideration is an accelerator with magnetic optics, RF cavities, and energy absorbers designed to maintain average beam energy while reducing the transverse momentum spread caused by energy loss in the absorbers. At the same time, the beam is reheated by scattering and stochastic effects. This is also true with Van der Meer cooling where the particle is heated by interactions with the other particles in the beam and by noise due to the electrons in the cooling system [5].

We model a quadrupole cooling channel with a standard though large bore FODO lattice [7] using the beam dynamics code COSY INFINITY [8,9] driven by the parameters of an absorber design from an sFOFO cooling channel design study [2].

2. Stochastic processes

The channel component that introduces stochastic processes in our simulations is the

*Corresponding author.
E-mail addresses: derrede@uiuc.edu (D. Errede), makino@uiuc.edu (K. Makino), berz@msu.edu (M. Berz), cjj@fnal.gov (C.J. Johnstone), vangin@fnal.gov (A. Van Ginneken).

0168-9002/$ - see front matter © 2003 Published by Elsevier B.V.
doi:10.1016/j.nima.2003.11.187

absorber. Muons of momentum range 150–400 MeV/c pass through the absorber to reduce the total momentum, hence both longitudinally and transversely, only to be reaccelerated in the RF cavities. The acceleration increases the longitudinal momentum component only. The total effect is to decrease the transverse momentum spread. The absorber produces not only momentum cooling but also reheats the beam transversely by multiple scattering from the nuclei in the absorber and longitudinally by straggling from the range in the energy loss distribution. As can be seen in Eq. (1), which describes [10] the rate of change in transverse normalized emittance ε_n with pathlength s,

$$\frac{d\varepsilon_n}{ds} = -\frac{1}{\beta^2}\frac{dE_\mu}{ds}\frac{\varepsilon_n}{E_\mu} + \frac{1}{\beta^3}\frac{\beta_\perp (0.014)^2}{2E_\mu m_\mu L_R} \quad (1)$$

the energy loss term reduces the emittance while the multiple scattering term produces an increase. E_μ is the kinetic energy of the muon and $\beta = v/c$. The ionization energy loss per unit length in the absorber is represented by dE_μ/ds. $\beta_\perp$ is the transverse beta function of the magnetic optics. The material radiation length L_R suggests using a substance with large radiation length such as liquid hydrogen, yet, sufficiently dense so that the energy losses remain substantial. The design and construction of this cooling channel component is important to the performance of the overall machine. The roughly cylindrical absorber is situated away from the RF cavities between two quadrupoles in a region of low magnetic and electric fields. The precise geometry to be implemented in a final cooling channel is still under design. Two aluminum windows of thickness 300 μm at the center enclose a volume of liquid hydrogen which was chosen for its low atomic number Z and the resulting decrease in multiple scattering. The exact properties are subject to change but the physical representation chosen for our simulations represents the absorber energy loss behavior to within an average of a few percent and to within a maximum of 10% of a design which includes a torospherical window [11] presently under consideration (Fig. 1). The simple model used for multiple scattering and energy loss is justified below.

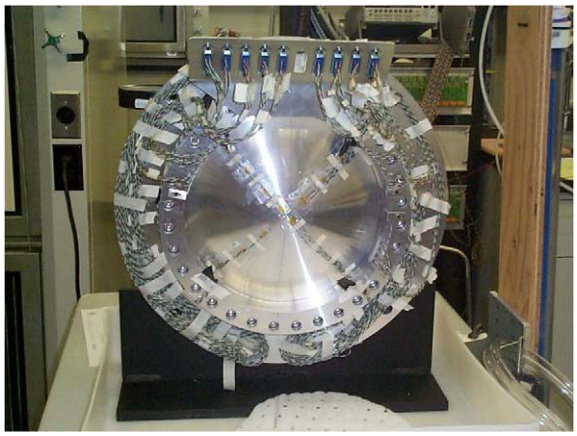

Fig. 1. Example of a torospherical window for sFOFO-type absorber in testing phase.

The multiple scattering probability P of the muon in the absorber is represented by Gaussians in both x and y.

$$P(\theta_x) = \frac{1}{\sqrt{2\pi\sigma^2}} e^{-(\theta_x^2/2\sigma^2)} \quad (2)$$

where θ_x is the scattering angle and σ^2 the variance.

$$\sigma^2 = \left(\frac{14\,\text{MeV}}{p\beta}\right)^2 \sum_i \frac{s_i}{L_{Ri}} \quad (3)$$

where i refers to the different materials along the absorber pathlength s, p the momentum and β the velocity of the charged particle (muon) and L_R is the radiation length. For the specific case under consideration the materials are hydrogen and aluminum. This yields a standard deviation $\sigma = 1^\circ$ for a muon of momentum 200 MeV/c. It is assumed that the variation in pathlength through the absorber for different orbits is small, hence s_i is assumed constant. The variance changes by 25% for the momentum range of interest. The small changes in the calculated distribution standard deviation due to velocity spread of the beam are ignored. Neglecting the logarithmic term in the multiple scattering formula is justified by an analysis of beryllium targets from a charm photoproduction experiment which demonstrates that the Gaussian representation (Rossi formula) fits the charm mass reconstruction as well as that using the logarithmic formulation [12]. Multiple

scattering from the two aluminum windows at their centers is small compared to that produced by the liquid hydrogen contained in the vessel. Near the outer radius the thickness is 2.4 mm. Here, the scattering from aluminum is comparable to that produced by the pathlength through hydrogen.

At the front end of the cooling channel the emittance is the largest. The smallest emittance blowup produced by window multiple scattering occurs at the front end due to the beam muons angular spread bounded above by the quadrupole channel angular acceptance of $\sim 20^\circ$. As the beam reaches its final emittance, limited by multiple scattering and energy straggling, the beam at the absorber is encompassed by a circle of radius ~ 14 cm, where the window thickness is smaller and, again, where the multiple scattering is small compared to that produced by the liquid hydrogen. Two flat aluminum windows that are 300 μm thick in the middle extended out to the outer radius and a cylinder of length 35 cm filled with liquid hydrogen represents the effects of energy loss and multiple scattering of a true absorber design well enough for our purposes. Regarding energy loss, this is so because in the actual design under consideration for the channel the increase in aluminum pathlength at the outer edges is partially compensated for by the reduction in hydrogen pathlength.

In order to fully describe the behavior of the muons in the cooling channel, the average energy loss and energy loss distribution are taken into account. The average energy loss is described by the Bethe–Bloch formula [13],

$$\frac{\mathrm{d}E}{\mathrm{d}x} = 2\pi N_\mathrm{a} r_\mathrm{e}^2 m_\mathrm{e} c^2 \rho \frac{Z}{A}\frac{z^2}{\beta^2} \times \left[\ln\left(\frac{2m_\mathrm{e}\gamma^2 v^2 W_\mathrm{max}}{I^2}\right) - 2\beta^2 - \delta - 2\frac{C}{Z}\right] \quad (4)$$

which includes two corrections. The density effect [14], which manifests itself in the quantity δ, is attributed to polarization of the medium thereby shielding the interaction of the muon with distant electrons. The effect is most important at higher energies past the minimum energy in the Bethe–Bloch equation. The second effect is the shell correction [15], reflected in the quantity C, which arises from the breakdown of the Bethe–Bloch formula assumption that the atomic electron is stationary with respect to the incoming particle. This contributes most strongly in the low-energy region, before the Bethe–Bloch minimum though the effect is small. It is noted that any possible longitudinal cooling brought about by setting the beam momentum above the Bethe–Bloch minimum is destroyed by energy loss fluctuations [16].

The average energy loss is insufficient to fully describe changes in energy of the beam. There is an energy loss distribution which varies as a function of the absorber thickness and muon velocity for a given type of absorber medium. The shape of this distribution can be categorized by the parameter κ, which is the ratio of the average total energy loss through the medium to the maximum energy lost per collision of the muon with an electron of the medium W_max, a kinematic limit that depends on the incoming particle momentum. The parameter κ increases with absorber thickness, but, is also a function of the velocity of the muon; κ varies inversely with the muon's momentum. For $\kappa < 10$ the energy loss distribution is in the non-Gaussian regime. With our absorber of thickness 35 cm and a muon momentum around 200 MeV/c, κ falls into the non-Gaussian regime and is best described by a theory of Symon [17] and Vavilov [18]. For thin absorbers and $\kappa < 0.01$, Landau's energy loss theory is applicable but the Vavilov formulation reduces to this in the limit of small κ. The spin $\frac{1}{2}$ of the muon has been included in the Vavilov distribution [16]; the effect is small and largest above the peak of the distribution as seen in Fig. 2.

The Vavilov energy distribution was implemented in the following way. The distribution was calculated for a muon momentum of 200 MeV/c. The distributions were then scaled only slightly by the average energy loss for different momenta (150–400 MeV/c). The shape of the distribution changes very little in this momentum region as can be seen by examining Figs. 3–6. In the case of 300 μm of aluminum the total energy loss is 0.14 MeV per window, which is small relative to 10.85 MeV lost in the hydrogen. Therefore the aluminum distribution is ignored and the average

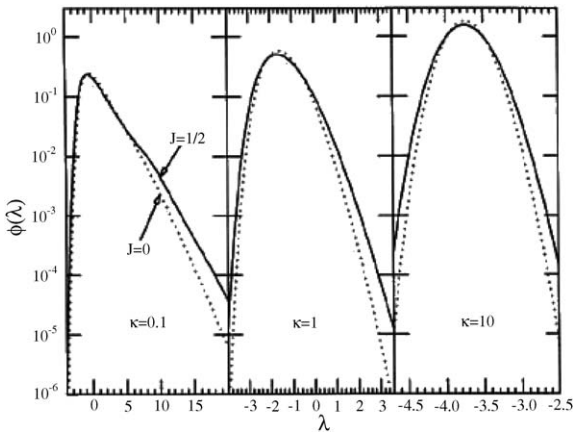

Fig. 2. Comparison of Vavilov distributions for spin 0 and $\frac{1}{2}$ for $\beta = 1$ and for different values of κ. See Ref. [16].

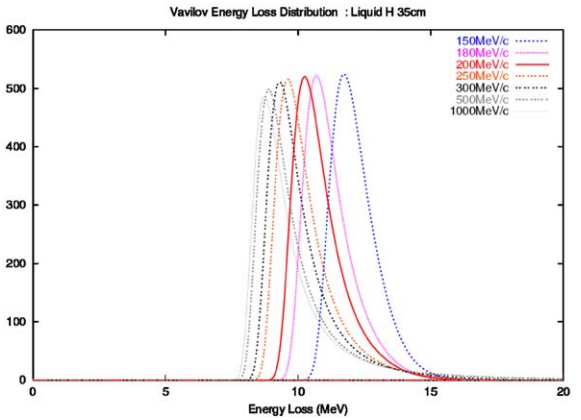

Fig. 3. Vavilov energy loss distribution for muons of momentum range 150–1000 MeV/c traversing 35 cm of liquid hydrogen.

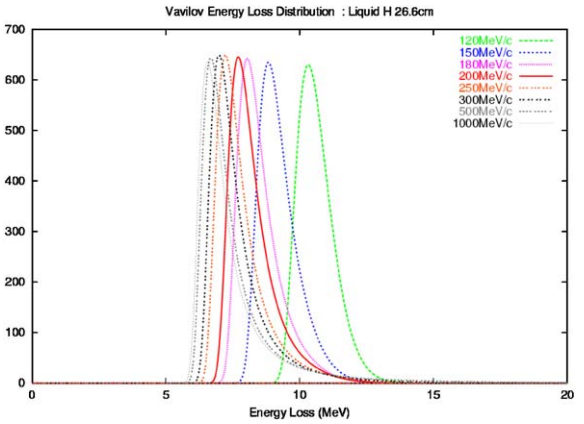

Fig. 4. Vavilov energy loss distribution for muons of momentum range 150–1000 MeV/c traversing 26 cm of liquid hydrogen.

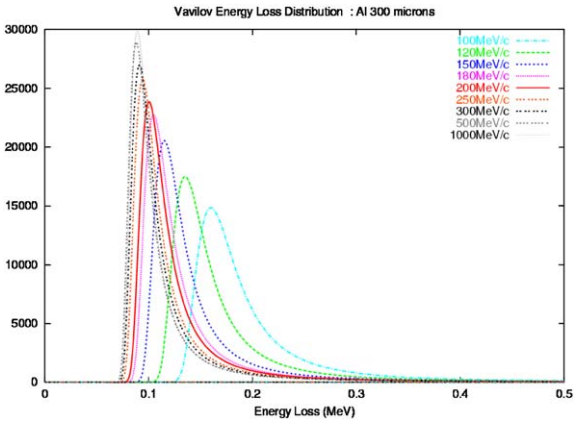

Fig. 5. Vavilov energy loss distribution for muons of momentum range 150–1000 MeV/c traversing 300 μm of aluminum.

energy loss is added to the total energy lost in the hydrogen. Also from Fig. 7 we see that the average energy loss as a function of beam momentum for the hydrogen and aluminum pathlengths for the absorber design under consideration at thicknesses that correspond to particles traversing straight through at the inner and outer radii compensate such that both loss calculations are within 10% of each other. In the COSY code the muon's momentum magnitude and direction are modified appropriately in the center of the absorber according to the appropriate Vavilov energy and Gaussian scattering distributions.

3. Beam cooling

As the beam particle energy loss provides cooling, the energy loss fluctuations increase the longitudinal phase-space volume, and multiple Coulomb scattering, increases the transverse phase-space volume, a delicate balance must be cut between choices of material, thicknesses of structures, and design of the quadrupole lattice. In fact, the progress of cooling can be seen by the graphs of emittance versus lattice cell number in Figs. 8–10. In Fig. 8 the emittances in both x and y reduce by a factor of two in 15 cells starting from

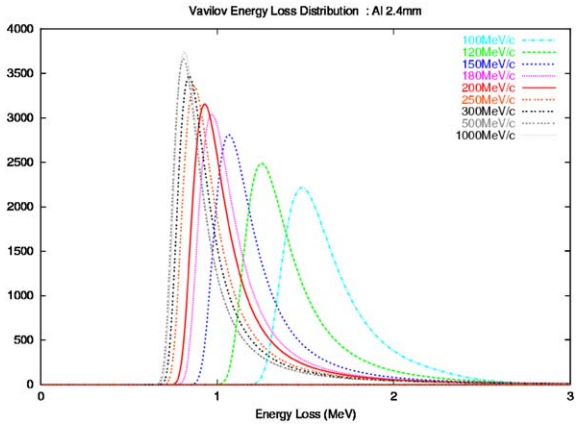

Fig. 6. Vavilov energy loss distribution for muons of momentum range 150–1000 MeV/c traversing 2.4 mm aluminum.

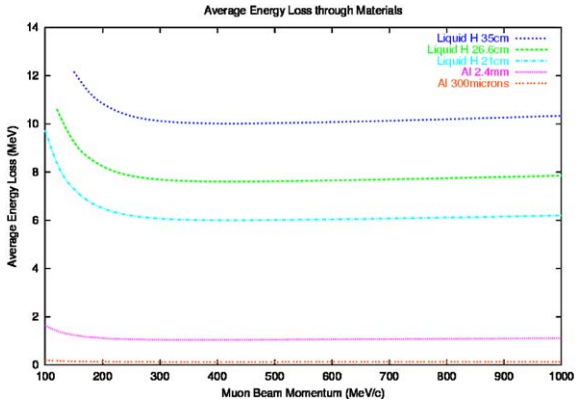

Fig. 7. Average energy loss as a function of beam momentum for different thicknesses of liquid hydrogen and aluminum.

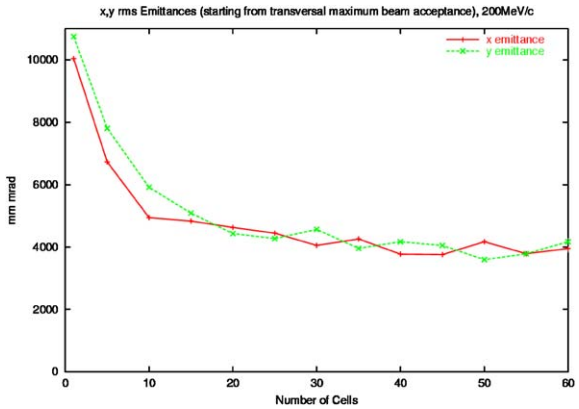

Fig. 8. Transverse emittance as a function of number of cells of quadrupole FODO lattice traversed starting at maximum transverse beam acceptance.

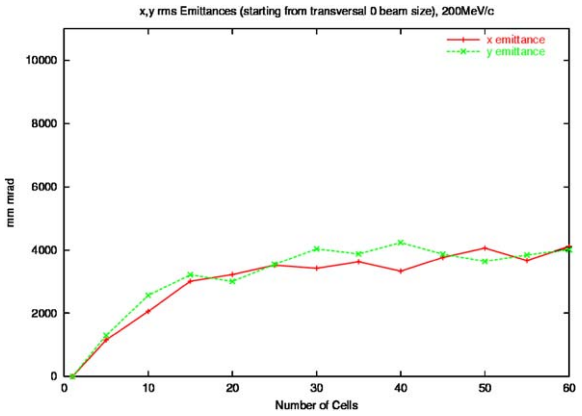

Fig. 9. Transverse emittance as a function of number of cells of quadrupole FODO lattice traversed starting at transverse beam positions $x = y = 0$.

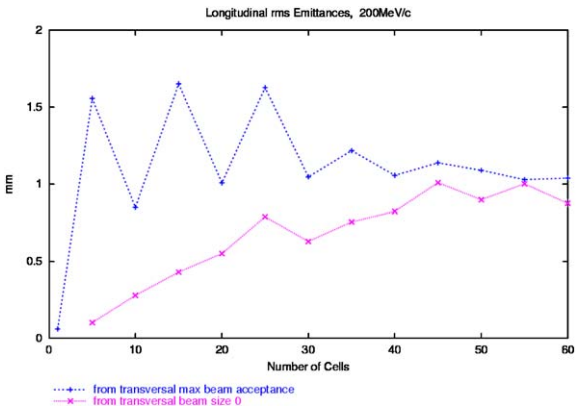

Fig. 10. Longitudinal emittance starting at both maximum and minimum transverse beam acceptance.

the maximum beam transverse acceptance for muons of the nominal momentum, 200 MeV/c. Fig. 9 demonstrates that the same equilibrium emittance is reached for particles launched with vanishing emittance (Fig. 10). The longitudinal emittance reaches equilibrium when particles are launched from both the vanishing emittance and maximum accepted emittance. Eq. (1), represents the change in transverse emittance as a function of position, s, along the orbit. It is minimized when the first term, a cooling term due to ionization energy loss, equals the second term, a heating term due to multiple scattering of the muons by the Coulomb force from the medium's nuclei (hydrogen in this case). Setting Eq. (1) equal to zero and

solving for ε_n yields the equilibrium emittance.

$$\varepsilon_{\min} = \frac{1}{\beta}\frac{\beta_\perp (0.014)^2}{2(\mathrm{d}E_\mu/\mathrm{d}s)m_\mu L_R} \quad (5)$$

- One minimizes $\beta_\perp$ by a suitable choice of the Hamiltonian within the practical constraints of the system under consideration; specifically this requires focusing elements of short focal length and large aperture. In practice, this is achieved either by the focusing properties of large aperture solenoids [2], or pairs or triplets of quadrupoles.
- The ionization energy loss, $\mathrm{d}E_\mu/\mathrm{d}s$, is velocity dependent, (see Eq. (2)) thus emittance minimization requires a proper choice of β again within the practical constraints of the system.
- The emittance is inversely proportional to the radiation length of the absorber medium thus materials with low density improve cooling performance.

It should be noted that the parameters for this channel and implementations are not yet optimized. For example, at this stage it is assumed that the magnetic field is zero in the absorber. Since the total acceleration design input and output to the cooling channel is not yet optimized this is not yet necessary.

4. Concluding remarks

The absorber introduces stochastic processes into the otherwise deterministic system represented by computational code. Those processes, energy loss and multiple scattering, are in turn represented by the Vavilov distribution and the Gaussian distribution, respectively. These processes are important in determining the limiting final equilibrium emittance of any cooling channel design. It is shown that the quadrupole FODO lattice cooling channel with these stochastic processes included does cool a beam of muons in the momentum range pertinent to this design.

Acknowledgements

This work was supported by the Illinois Consortium for Accelerator Research, the Department of Energy, and the National Science Foundation.

References

[1] N. Holtkamp, D. Finley, (Eds.), A feasibility study of a neutrino source based on a muon storage ring, Fermilab-Pub-00/108-E, 2000; http://www.fnal.gov/projects/muon-collider/nu-factory/nu-factory.html.
[2] S. Ozaki, R. Palmer, M. Zisman, J. Gallardo, (Eds.), feasibility study-II of a muon-based neutrino source, BNL-52623.
[3] A. Skrinsky, Colliding beams program in Novosibirsk. International Seminaron Prospects in High Energy Physics, Morges, 1971.
[4] G.I. Budker, Colliding beams prospects, XV International Conference on High Energy Physics, Kiev, 1970.
[5] F.T. Cole, F.E. Mills, Annu. Rev. Nucl. Part. Sci. 31 (1981) 295.
[6] S. Van der Meer, Stochastic damping of betatron oscillations in the ISR, CERN/ISR-PO/72-31, 1972.
[7] C.J. Johnstone, M. Berz, D. Errede, K. Makino, Muon beam ionization cooling, Nucl. Instr. and Meth. A, these proceedings.
[8] M. Berz, K. Makino. COSY INFINITY, Version 8.1—User's Guide and Reference Manual, Technical Report MSUHEP-20704, Department of Physics and Astronomy, Michigan State University, East Lansing, MI 48824, 2001; see also http://cosy.pa.msu.edu.
[9] K. Makino, M. Berz, D. Errede, C.J. Johnstone, Higher order map treatment of superimposed cavities, absorbers, and magnetic multipole and solenoid fields. Nucl. Instr. and Meth. A these proceedings.
[10] D. Neuffer, Nucl. Instr. and Meth. A 362 (1995) 213.
[11] D.M. Kaplan, et al., Progress in energy absorber R&D 2: windows, Proceedings of the 2001 Particle Accelerator Conference, 3888.
[12] J. Wiss, Department of Physics, University of Illinois, Urbana-Champaign, Illinois, personal communication.
[13] W.R. Leo, Techniques for Nuclear and Particle Physics Experiments: A How-to Approach, Springer, New York, 1987, pp. 1994.
[14] R.M. Sternheimer, M.J. Berger, S.M. Seltzer, Atom Data Nucl. Data Tables 30 (1984) 262.
[15] W.H. Barkas, M.J. Berger, Tables of energy losses and ranges of heavy charged particles, in: Studies in the Penetration of Charged Particles in Matter, National Academy of Sciences Publication 1133, Nuclear Science Series Report No. 39, 1964.
[16] A. Van Ginneken, Nucl. Instr. and Meth. A 362 (1995) 213.
[17] K.R. Symon, Fluctuations in energy loss by high energy charged particles in passing through matter, Thesis, Department of Physics, Harvard University, Cambridge, MA, 1948.
[18] P.V. Vavilov, Sov. Phys.-JETP 5 (4) (1957) 749.